Numerical Dispersion

Review of Linear Numerical Stability

In the previous lecture, we considered the linear numerical stability of both advection and diffusion terms when approximated with several spatial and temporal differencing schemes. To determine the linear stability of the advection equation, we assumed that a model variable h has wave-like solutions of the form $h = \hat{h}e^{i(kx-\omega t)}$, where $\hat{h}$ is amplitude, k is a zonal wavenumber, L is wavelength, and $\omega = Uk$ is frequency. The frequency has both real and imaginary components, i.e., $\omega = \omega_R + i\omega_I$, such that $h = \hat{h}e^{\omega_I t}e^{i(kx-\omega_R t)}$. Thus, the amplitude of h may change with time as a function of the value of $e^{\omega_I}t$.

Finite difference schemes may be absolutely stable, conditionally stable, or absolutely unstable. For absolutely unstable schemes, the model solution will grow exponentially for all chosen values of the parameters that determine its numerical stability. Conversely, for absolutely stable schemes, the model solution will remain stable for all chosen values of the parameters that determine its numerical stability. For conditionally stable schemes, however, the model solution will remain stable so long as the chosen values of the parameters that determine its numerical stability adhere to the stability criterion for the chosen differencing scheme.

To determine linear stability, we considered a one-dimensional advection equation of the form:

$$\left.\frac{\partial h}{\partial t}\right|_j^\tau = -U\left.\frac{\partial h}{\partial x}\right|_j^\tau$$

We then discretized this equation using various combinations of spatial and temporal finite difference approximations. The resulting equation was then solved for $|e^{\omega_I\Delta t}|$, noting that $e^{\omega_I t} = \left(e^{\omega_I\Delta t}\right)^\tau$ given $t = \tau\Delta t$ and τ = time step number.

We found that the forward-in-time, backward-in-space finite difference scheme is *conditionally stable*. When the stability condition is satisfied, the model solution is exponentially damped with time. This exponential damping is a function of wavelength, with shorter wavelengths associated with the greatest damping, and the Courant number, with intermediate stable values of the Courant number associated with the greatest damping. However, the centered-in-time, 2nd order centered-in-space and centered-in-time, 4th order centered-in-space finite difference schemes, while also being conditionally stable, are not associated with exponential damping.

Intuitively, shorter wavelength features – where Δx is large relative to their wavelength L – are poorly resolved on the model grid. Two lectures ago, we demonstrated that shorter wavelength features are associated with relatively large truncation error compared to their longer wavelength counterparts. As we will see in this and the next lecture, shorter wavelength features are also problematic with respect to their modeled propagation and their non-linear interactions with other

short wavelength features in the model. Consequently, the damping of such features, whether via the chosen finite difference scheme or explicit numerical diffusion, is often desired to improve the quality of the model solution.

In this lecture, we introduce the concept of numerical dispersion, describing non-physical wave and energy propagation that can result from finite differencing schemes, and demonstrate that it is particularly troublesome for short wavelength features.

Numerical Dispersion

Consider the linear one-dimensional advection equation stated above. The advective speed of the wave defined by h is simply equal to U, a constant advective velocity. More precisely, the phase speed of any wave – defining its motion – is given by:

$$C_p = \frac{\omega}{k}$$

Here, since $\omega = Uk$, $C_p = U$. Likewise, the group velocity of any wave – defining the propagation of the wave's energy – is given by:

$$C_g = \frac{\partial \omega}{\partial k}$$

Here, again since $\omega = Uk$, $C_g = U$. Because $C_p = C_g$, the wave is said to be *non-dispersive*. This is true of any advective wave in nature. To prove this, consider the linear one-dimensional advection equation stated above and the general solution for h of the form $h = \hat{h}e^{i(kx-\omega t)}$. Plugging this in and solving for the partial derivatives analytically, we obtain:

$$-i\omega\hat{h}e^{i(kx-\omega t)} = -ikU\hat{h}e^{i(kx-\omega t)}$$

This simplifies to the $\omega = Uk$ expression that was stated without derivation above.

When the solution to the advection equation is approximated using finite difference schemes, the phase speed and group velocity may not necessarily equal U, nor will they necessarily equal each other. Rather,

$$C_p = \frac{\omega_R}{k} \qquad \text{and} \qquad C_g = \frac{\partial \omega_R}{\partial k}$$

Consider, for instance, the forward-in-time, backward-in-space finite difference scheme applied to the one-dimensional advection equation. In our previous lecture, we found that:

$$e^{\omega_I \Delta t}\left(\cos(\omega_R \Delta t) - i\sin(\omega_R \Delta t)\right) - 1 = -\frac{U\Delta t}{\Delta x}\left(1 - \left(\cos(k\Delta x) - i\sin(k\Delta x)\right)\right)$$

Separating this equation into its real (top) and imaginary (bottom) components, we obtained:

$$e^{\omega_I \Delta t}\cos(\omega_R \Delta t) = 1 - \frac{U\Delta t}{\Delta x}\left(1 - \cos(k\Delta x)\right)$$

$$e^{\omega_I \Delta t}\sin(\omega_R \Delta t) = \frac{U\Delta t}{\Delta x}\sin(k\Delta x)$$

To evaluate the linear numerical stability of this scheme, we solved the system of equations for $e^{\omega_I \Delta t}$ by eliminating ω_R. To determine the phase speed and group velocity of this scheme, we now wish to solve the system of equations for ω_R by eliminating $e^{\omega_I \Delta t}$. We can do so by dividing the bottom equation by the top equation to obtain:

$$\frac{\sin(\omega_R \Delta t)}{\cos(\omega_R \Delta t)} = \frac{\dfrac{U\Delta t}{\Delta x}\sin(k\Delta x)}{1 - \dfrac{U\Delta t}{\Delta x}\left(1 - \cos(k\Delta x)\right)}$$

To solve this equation for ω_R, note that the left-hand side of the above equation is simply equal to $\tan(\omega_R \Delta t)$. Thus, take the inverse tangent (or arctangent) of both sides to obtain:

$$\omega_R \Delta t = \arctan\left(\frac{\dfrac{U\Delta t}{\Delta x}\sin(k\Delta x)}{1 - \dfrac{U\Delta t}{\Delta x}\left(1 - \cos(k\Delta x)\right)}\right)$$

For $\omega_R = C_p k$, we can rewrite the above equation as:

$$C_P = \frac{1}{k\Delta t}\arctan\left(\frac{\dfrac{U\Delta t}{\Delta x}\sin(k\Delta x)}{1 - \dfrac{U\Delta t}{\Delta x}\left(1 - \cos(k\Delta x)\right)}\right)$$

It is clear that the phase speed is not simply equal to U but is now dependent upon the model time step Δt, the grid spacing Δx, and the wavelength L (since $k = 2\pi/L$). This dependency is visualized in Figure 1. (Note that depicted in Figure 1 is the ratio of the approximate C_p to the exact advective velocity U, similar to the methodology used to visualize truncation error – approximate divided by exact solution.)

For waves of wavelength $5\Delta x$ and longer, the phase speed is slower than U for $C < 0.5$, equal to U for $C = 0.5$ and 1, and greater than U for $0.5 < C < 1$. As we determined in the previous lecture,

this finite difference scheme is unstable for $C > 1$. For waves of wavelength $4\Delta x$ and shorter, the phase speed is again slower than U for $C < 0.5$ and equal to U for $C = 0.5$. However, for larger values of C, the phase speed can be negative – or, in the case of the $4\Delta x$ wave, undefined when $C = 1$. Note that this is different than is depicted in Figure 3.24 of the course text, upon which Figure 1 is based; this represents an error in the course text, which one can prove by obtaining C_p oneself using the above equation for Courant numbers between 0.5 and 1.
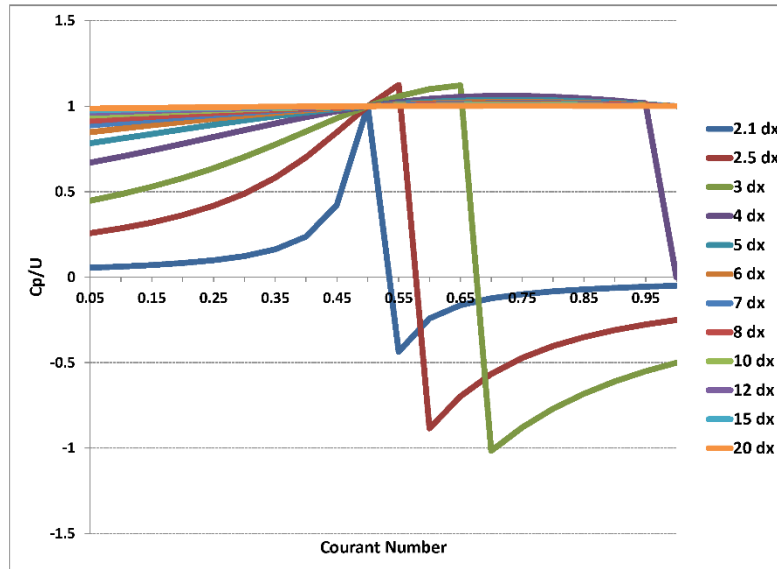

Figure 1. Ratio of the phase speed C_p to the advective velocity U for the forward-in-time, backward-in-space finite difference scheme applied to the one-dimensional advection equation for Courant numbers C between 0.05 and 1 and waves of wavelength between $2.1\Delta x$ and $20\Delta x$. Adapted from Warner (2011), their Figure 3.24, with correct data plotted for wavelengths $\leq 4\Delta x$.

The dependency of the phase speed upon wavelength indicates that the wave-like solution for h is *dispersive*. In general, a wave with a phase speed that depends upon wavelength is dispersive. We will consider what this means conceptually with an example later in this lecture. Similarly, one could take the equation for $\omega_R \Delta t$, solve it for ω_R, and then take its first partial derivative with respect to k to obtain an expression for C_g, the group velocity describing wave energy propagation. Doing so, one would find that $C_p \neq C_g$, such that the wave and its energy are associated with different propagation characteristics, a characteristic of a dispersive wave.

The process described above for the forward-in-time, backward-in-space finite difference scheme can be repeated for *any* finite difference scheme. For example, doing so for the centered-in-time, 2nd order centered-in-space finite difference scheme, it can be shown that:

$$\omega_R \Delta t = \arcsin\left(\pm \frac{U\Delta t}{\Delta x} \sin(k\Delta x) \right)$$

Substituting for $\omega_R = C_p k$, we can rewrite the above equation as:

$$C_p = \frac{1}{k\Delta t}\arcsin\left(\pm\frac{U\Delta t}{\Delta x}\sin(k\Delta x)\right)$$

Because of the $\pm$ symbol, there are two different phase speeds – for two different waves – defined above:

$$C_p = \frac{1}{k\Delta t}\arcsin\left(\frac{U\Delta t}{\Delta x}\sin(k\Delta x)\right)$$

$$C_p = \frac{1}{k\Delta t}\arcsin\left(-\frac{U\Delta t}{\Delta x}\sin(k\Delta x)\right)$$

The first is an approximation to the physical wave that moves in the same direction as, but at a slower rate of speed than, the physical wave. The second is a fictitious wave, or *computational mode,* that moves in the opposite direction of with smaller magnitude than the physical wave. The ratios of the phase speed C_p to the advective velocity U for each wave are plotted in Figure 2. Note that the greatest departures from $|U|$ occur for $L < 8\Delta x$ and for smaller Courant numbers.
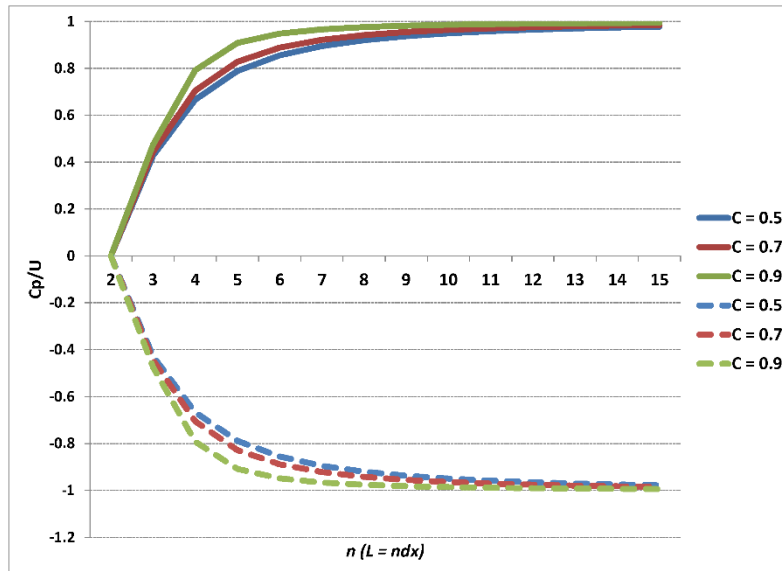

Figure 2. Ratio of the phase speed C_p to the advective velocity U for the centered-in-time, 2nd order centered-in-space finite difference scheme applied to the one-dimensional advection equation as a function of wavelength for three selected values of the Courant number. Solid lines depict the phase speed of the approximation to the physical wave while dashed lines depict the phase speed of the computational mode. Adapted from Warner (2011), their Figure 3.25.

Generally speaking, a temporal differencing scheme that involves computations at more than two times (e.g., the current and future times) will result in one or more computational modes. For example, the centered-in-time temporal differencing scheme is 2nd order accurate – involving three times – and has one physical mode and one computational mode. The Runge-Kutta 3 temporal differencing scheme is 3rd order accurate – involving four times – and has one physical mode and two computational modes. In general, for a temporal differencing scheme that is N^{th} order accurate, involving $N+1$ times, there are $N-1$ computational modes.

The computational mode(s) typically have much smaller amplitude than does the physical mode. It can be difficult to isolate the impact of the computational mode upon the numerical solution from that of wave dispersion. As depicted above, wave dispersion is most evident for shorter wavelength features; this is generally true for computational mode solutions as well.

Typically, both computational mode and short wavelength dispersive waves are dampened in the model solution by some means. Implicit numerical diffusion, which we discussed indirectly in the last lecture, and explicit numerical diffusion, which we will discuss more in the next lecture, are two ways of damping these waves. Time filtering may also be used to mitigate the computational mode, but this typically also reduces the accuracy of the temporal differencing scheme and is associated with a more stringent stability criterion than if it were not used.

Returning to the centered-in-time, 2nd order centered-in-space differencing scheme, we can obtain the group velocity C_g for the approximation to the physical wave. To wit,

$$C_g = \frac{\partial \omega_R}{\partial k} = \frac{\partial (C_p k)}{\partial k}$$

If we plug in for C_p, we obtain:

$$C_g = \frac{\partial}{\partial k}\left(\frac{1}{\Delta t}\arcsin\left(\frac{U\Delta t}{\Delta x}\sin(k\Delta x)\right)\right)$$

Noting that:

$$\frac{\partial}{\partial k}\arcsin(a(k)) = \frac{1}{\sqrt{1-a^2}}\frac{\partial a}{\partial k}$$

we obtain:

$$C_g = \frac{1}{\Delta t}\left(\frac{1}{\sqrt{1-\left(\frac{U\Delta t}{\Delta x}\sin(k\Delta x)\right)^2}}\right)\frac{\partial}{\partial k}\left(\frac{U\Delta t}{\Delta x}\sin(k\Delta x)\right)$$

Such that:

$$C_g = \frac{1}{\Delta t}\left|\frac{\dfrac{U\Delta t}{\Delta x}\Delta x\cos(k\Delta x)}{\sqrt{1-\left(\dfrac{U\Delta t}{\Delta x}\sin(k\Delta x)\right)^2}}\right|$$

Simplifying, we obtain:

$$C_g = \left|\frac{U\cos(k\Delta x)}{\sqrt{1-\left(\dfrac{U\Delta t}{\Delta x}\sin(k\Delta x)\right)^2}}\right|$$

The ratio of the group velocity to the advective velocity is depicted in Figure 3. Whether viewed mathematically or in terms of actual values (c.f. Figures 2 and 3), the group velocity and phase speed are not equal, such that the propagation of the wave and its energy are not coincident with each other. For $L < 4\Delta x$, the group velocity is in the opposite direction of the wave's propagation. For $L = 4\Delta x$, the group velocity is stationary. For $L > 4\Delta x$, the group velocity is in the same direction as but slower than the wave's propagation, particularly for $L < {\sim}10\Delta x$. As with phase speed, the greatest departures from $|U|$ occur for smaller values of the Courant number.
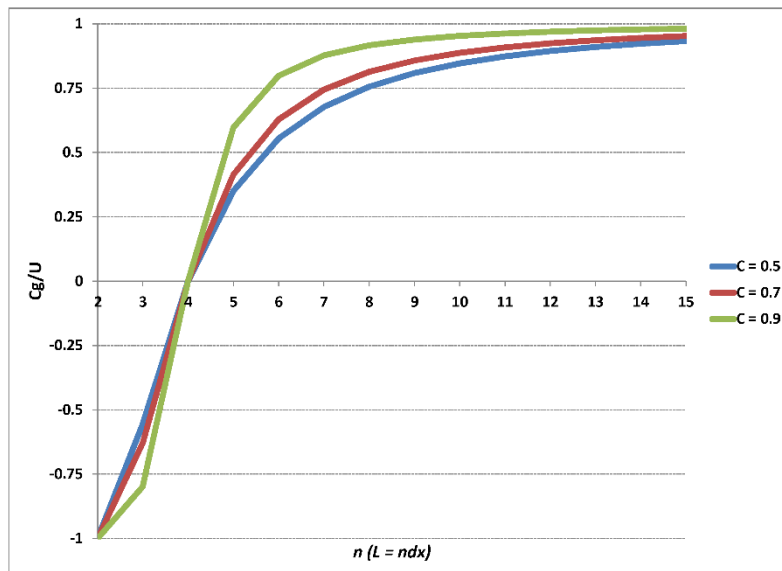

Figure 3. Ratio of the group velocity C_g to the advective velocity U for the centered-in-time, 2nd order centered-in-space finite difference scheme applied to the one-dimensional advection

equation as a function of wavelength for three selected values of the Courant number. Adapted from Warner (2011), their Figure 3.25.

Note that the wavelength- and Courant number-dependence of C_p and C_g will vary between finite differencing schemes.

An Example

Consider a model that solves the one-dimensional advection equation given by:

$$\frac{\partial h}{\partial t} = -U \frac{\partial h}{\partial x}$$

Let the model grid contain 100 grid points. Use periodic boundary conditions, such that grid point 1 is adjacent to grid points 100 and 2, and grid point 100 is adjacent to grid points 99 and 1. Here, we let $\Delta x = 1$ km (such that the domain length is 100 km) and $U = 10$ m s^{-1}. The initial h is defined by a short wavelength Gaussian wave, with high amplitude for large k and low amplitude for small k, in the height field at the center of the model grid.

We consider three model time steps: $\Delta t = 10$ s, such that $C = 0.1$; $\Delta t = 50$ s, such that $C = 0.5$; and $\Delta t = 90$ s, such that $C = 0.9$. In each case, the model is integrated forward in time until the Gaussian-like wave returns to its original location (at $t = 100000$ m / 10 m s^{-1} = 10000 s); thus, the exact solution is identical to the initial condition. The centered-in-time, 2nd order centered-in-space finite differencing scheme is used for each integration; as a result, there is no implicit damping of the model solution with time for any value of C.
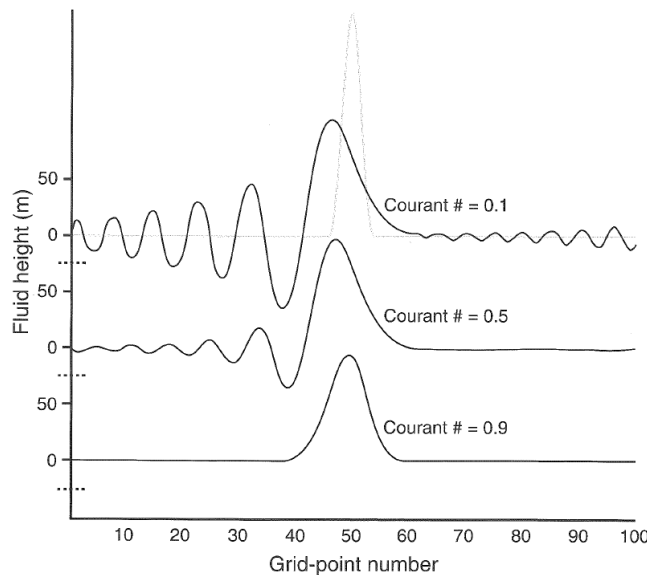
Figure 4. Fluid height h (m) after integrating the one-dimensional advection equation for 10,000 s on the model grid described in the text above for Courant numbers C of 0.1 (top), 0.5 (middle), and 0.9 (bottom). The thin grey curve in the top panel represents both the initial condition and exact solution. Reproduced from Warner (2011), their Figure 3.27.

In Figure 4, the approximate solution for each of the above-listed Courant numbers is depicted. The initial condition and exact solution are given by the thin grey line in the top panel.

Though we conceptualize the physical wave as a single wave, it is better conceptualized as the linear superposition of many waves of varying wavelength (e.g., as may be depicted using a Fourier series). Given our earlier analysis in Figure 2, we know that the phase speed of each individual wave differs from that of the others: shorter wavelength features move at a slower rate of speed than the longer wavelength features. For *all* wavelengths, this effect is smallest when the Courant number is ~1 and is magnified for smaller Courant numbers.

Now, consider the cases where $C = 0.1$ but centered-in-time, 4th order centered-in-space (Figure 5) and third-order Runge-Kutta in time, 6th order centered-in-space (Figure 6) finite differencing schemes are used. There is no implicit damping for the centered-in-time, 4th order centered-in-space scheme, but there is implicit damping of shorter wavelength features with time for the third-order Runge-Kutta in time, 6th order centered-in-space scheme due to the Runge-Kutta temporal differencing.
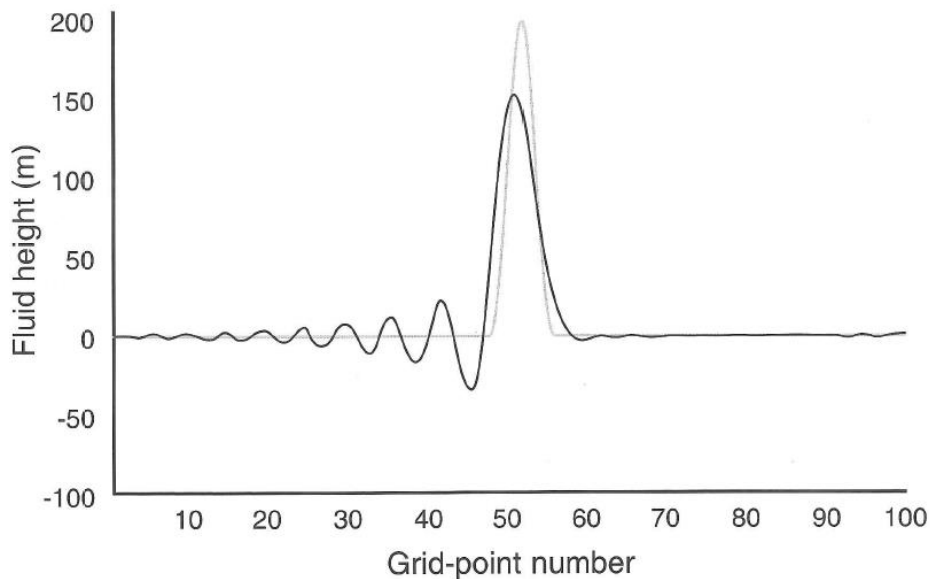

Figure 5. As in the top panel of Figure 4, except using the centered-in-time, 4th order centered-in-space finite differencing scheme. Reproduced from Warner (2011), their Figure 3.28.

In both cases, short wavelength features move slower than the physical wave, as was demonstrated above for the centered-in-time, 2nd order centered-in-space scheme. However, the amplitude of these shorter wavelength features in the more accurate schemes is reduced compared to that in the centered-in-time, 2nd order centered-in-space scheme. Consequently, the amplitude of the primary wave is better preserved. Thus, utilizing more accurate finite difference schemes in both time and space mitigates the deleterious effects of numerical dispersion upon the model solution.
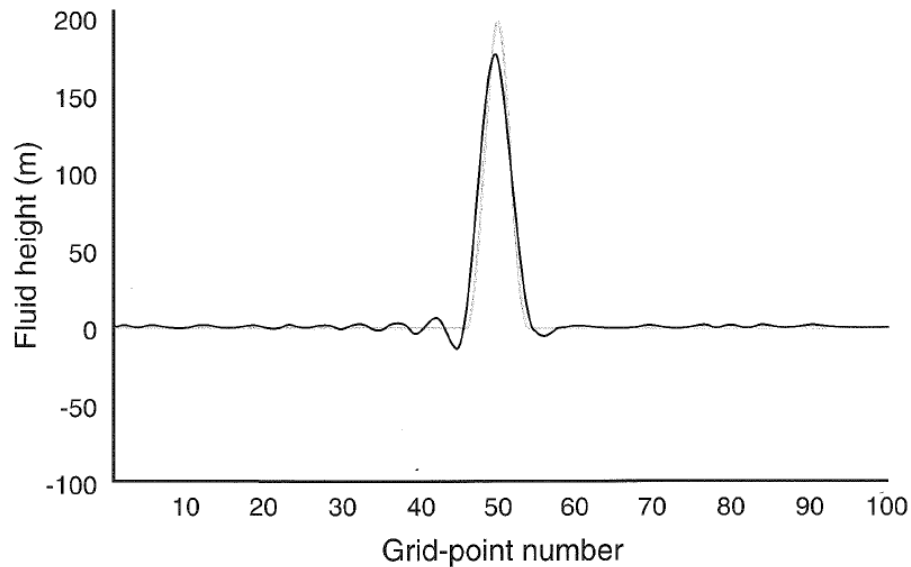

Figure 6. As in the top panel of Figure 4, except using the third-order Runge-Kutta in time, 6th order centered-in-space finite differencing scheme. Reproduced from Warner (2011), their Figure 3.30.